Prediction of the time to failure of boiler tubes flawed with localized erosion

Ifeanyi Emmanuel Kalu, Helen Mary Inglis, Schalk Kok
Centre for Asset Integrity Management, Department of Mechanical and Aeronautical Engineering, University of Pretoria, Hatfield, Pretoria, 0028, South Africa.

Abstract

A failure mechanism prevalent with boiler tubes operating in harsh environmental conditions is localized erosion. The consequence of the erosion mechanism is a substantial reduction of the tube thickness, ultimately leading to plastic collapse and consequently rupturing of the tubes. Locating and repairing all the affected tubes within the boiler is time consuming and expensive. It will be worthwhile to rank all the identified flaws so that critical flaws that cannot survive till the next scheduled shutdown are prioritized for repair. Consequently, nonlinear structural analysis was conducted on various boiler tubes that failed by localized erosion. The tubes had a wide range of localized erosion flaws that required a detailed assessment technique. The failure was evaluated numerically using various stress and strain-based failure criteria as well as performing the American Petroleum Institute and the American Society of Mechanical Engineers (API-ASME) fitness-for-service (FFS) assessment on the tubes. A projected time to failure (P_t) for each tube based on the various criteria used in this study was determined. This enabled the ranking of the flawed tubes based on the priority of their repair. The outcome of this study demonstrates the potential for a tool which will enable industry users to prioritise the replacement or repair of critically flawed tubes and avert replacing tubes that are still safe for future operation.

Keywords: Boiler tubes, nonlinear structural analysis, localized erosion, strain-based failure criteria, stress-based failure criteria, API-ASME FFS, failure prediction, projected time to failure.

1 Introduction

Boiler tubes are essential components of boilers, used to produce steam in manufacturing industries and power plants. The steam produced can be used to run machinery in a process plant or delivered to a turbine to generate electricity in power plants. Due to the high temperature and high pressure environment in which the tubes operate, they are predisposed to experiencing a broad-range of failures caused by overheating, corrosion, erosion, fatigue, material, manufacturing, and welding defects [1–5]. These damage mechanisms lead to deformation, thinning and bulging of the tubes, or formation of cracks, gouges, and pits, which eventually leads to the bursting of the tubes while in operation [1,3,6]. Prevalent among the reoccurring tube failures is localized thinning of the tubes driven by erosion [1–4,7].

Typically, in a power plant, localized external erosion of boiler tubes occurs due to prolonged abrasive interaction of the tube external surface with coal particles, falling slag and fly ash proceeding from the boiler's combustion chamber [1,3,8]. It can also occur due to the soot blower misdirecting steam at high velocity on the tubes, or steam cutting from a failed tube impinging on nearby tubes [2,3,9]. The protracted interaction of a tube with these failure drivers can result in a large, localized decrease in its wall thickness, leading to plastic collapse due to increased strain within the tubes, and hence to rupturing of the tubes [2,10,11]. As a result of tube failures, affected power or manufacturing plants would have to be shut down, thereby leading to unplanned boiler outages and repairs, as well as production loss [1–4,6,12–14]. Approximately 25% of all tube failures associated with fossil fuel power plants are caused by erosion [7], resulting in billions of dollars lost due to electricity loss and repair cost [2].

When a plant has to be shut down for normal maintenance activities or due to occurrence of tube leakages, all defected tubes should ideally be replaced or repaired. But because of insufficient time during the shutdown, it may only be possible to work on critically flawed

tubes. Moreover, in an environment with ageing infrastructure and with a tight budget, replacing defected tubes that can still be safe for continued service will not be financially prudent. Conversely, if flawed tubes that are critical are not replaced or repaired, there is a high risk of unplanned failures, production loss, forced outages, and inevitably expensive emergency repairs. Hence, there is a need to find a means to assess these tubes so that flawed tubes that cannot survive until the next shutdown are prioritized ahead of safe tubes.

Failure assessment of pressurized vessels, like boiler tubes, under localized erosion has been carried out using various strain and stress-based criteria. A 2% plastic strain ($P_{2\%}$) failure criterion was recommended for assessing round and groove shaped localized thinned flaws in pressurized vessels [15,16]. The use of ultimate tensile strength (σ_{uts}) of the pressurized vessel as a reference failure stress criterion has also been proposed [17–19]. In this case, failure of the vessel is considered when the peak von Mises equivalent stress equals σ_{uts}. Others have suggested 80% or 90% σ_{uts} [20,21] and flow strength (defined as an average of the yield strength σ_y and σ_{uts}) [4,21,22] as stress-based failure criteria. True ultimate tensile strength $(\sigma_{t,uts})$ has also been used as a reference failure stress for investigative studies [23,24]. Attempts have also been made to estimate the tube life based on flow strength and design stress of the tubes [4,25]. Localized erosion in boiler tubes continues to be a prevalent cause of tube leakages, leading to unplanned boiler outages in energy generation and process industries. Hence, the need for additional studies to aid in mitigating this challenging situation.

In this paper, assessment of a broad range of locally flawed boiler tubes was conducted and analysed using different stress and strain failure criteria to evaluate the failure of the tubes. Fitness-for-service (FFS) assessment was also carried out using the American Petroleum Institute and the American Society of Mechanical Engineers (API-ASME) FFS Standard. The assessment outcomes were compared to that of the stress and strain failure limits. As an extension of our previous work, [12], the projected time to failure for each of the tubes was

computed, demonstrating the potential of our method to guide industry users in categorizing observed flaws based on their estimated time to failure.

2 Assessment of boiler tubes due to localized erosion

2.1 Material properties

For the study, sixteen flawed boiler tubes that failed as a result of localized erosion are used. Table 1 summarizes the flaw dimensions. t is the thickness of the unflawed tube, D_o is the actual external diameter of the unflawed tube, f_l is the flaw length, f_w is the flaw width, and t_f is the remaining thickness of the failed tube, measured after shutdown.

The effect of temperature on the tubes' properties is considered as described in design codes. Using the BS 3059: Part 2 standard [26], the Young's modulus of elasticity, E, and coefficient of thermal expansion, α, with reference to temperature change for all the tubes can be seen in Table 2. A Poisson ratio of v = 0.3 is used for all the tubes. The strength properties of the tubes, specifically yield strength (σ_y) and ultimate tensile strength (σ_{uts}), with respect to temperature change are determined at the operating temperature using analytical expressions documented in Annex 2E.2.1.2 and 2E.2.1.3 of the API-ASME FFS standard [27]. Based on the strength values of the tubes at ambient temperature (T_a) and their respective operating temperatures (T), the calculated σ_y and σ_{uts} values at their corresponding operating temperatures are shown in Table 3.

Table 1
Boiler tube flaws used for the failure assessment.

Flaw Numbers	Tube Grades	t (mm)	D_o (mm)	f_l (mm)	f_w (mm)	t_f (mm)
1	15Mo3	5.6	44.5	225	35	0.41
2	15Mo3	6.5	33.9	300	30	0.24
3	15Mo3	5.2	44.5	140	44	0.50
4	15Mo3	3.6	33.0	20	15	0.20
5	SA 210 A1	6.3	50.8	150	50	0.38
6	SA 210 A1	5.4	47.5	400	45	1.20
7	BS 3059 Gr. 620	4.2	34.9	300	30	0.20

8	BS 3059 Gr. 440	3.8	38.0	500	35	0.45
9	BS 3059 Gr. 440	6.1	63.5	600	50	0.63
10	BS 3059 Gr. 440	5.4	63.0	310	60	0.42
11	BS 3059 Gr. 440	3.8	38.0	110	28	0.30
12	BS 3059 Gr. 440	3.8	38.0	155	32	0.30
13	BS 3059 Gr. 440	6.6	63.5	240	30	0.80
14	BS 3059 Gr. 360	4.4	50.8	70	40	0.17
15	BS 3059 Gr. 360	4.4	50.8	80	25	0.30
16	BS 3059 Gr. 360	7.0	75.0	600	20	0.50

Table 2

Boiler tube properties based on temperature changes [26,28].

Temperature (℃)	E (GPa)	α ($\times 10^{-6}$ ℃$^{-1}$)
20	212	11.50
100	206	11.90
200	198	12.60
300	191	13.10
400	183	13.70
500	174	14.10

Table 3

Boiler tube strength properties with reference to temperature.

Tube grades	σ_y (MPa) at T_a	σ_{uts} (MPa) at T_a	T (℃)	Computed σ_y (MPa) at T	Computed σ_{uts} (MPa) at T
15Mo3	270	450	370	242.32	403.87
15Mo3	270	450	400	241.17	401.95
15Mo3	270	450	405	240.88	401.46
15Mo3	270	450	414	240.27	400.45
SA 210 A1	255	415	390	183.56	298.74
SA 210 A1	255	415	400	181.91	296.04
BS 3059 Gr. 620	180	460	431	143.24	366.07
BS 3059 Gr. 440	245	440	250	197.33	354.39
BS 3059 Gr. 440	245	440	333	185.17	332.55
BS 3059 Gr. 440	245	440	350	182.59	327.92
BS 3059 Gr. 440	245	440	367	179.97	323.22
BS 3059 Gr. 440	245	440	417	172.03	308.95
BS 3059 Gr. 360	235	360	358	173.96	266.49
BS 3059 Gr. 360	235	360	384	170.08	260.54

The stress-strain curve model of the Material Properties Council (MPC) as documented in Annex 2E.3.1 of the API-ASME FFS [27] is used for the tube assessment. The model enables the strain hardening of the stress-strain curve to be taken into consideration. Prior studies have either not taken this into account [29,30] or have used elastic-perfectly plastic models [2,15,16]. By substituting in the computed material properties of the tubes at the operating temperature into the model, realistic strain hardening curves are developed for all the tubes. The generated true stress-strain curve for each tube as shown in Fig. 1 is then used for the mechanical analysis in ANSYS®.

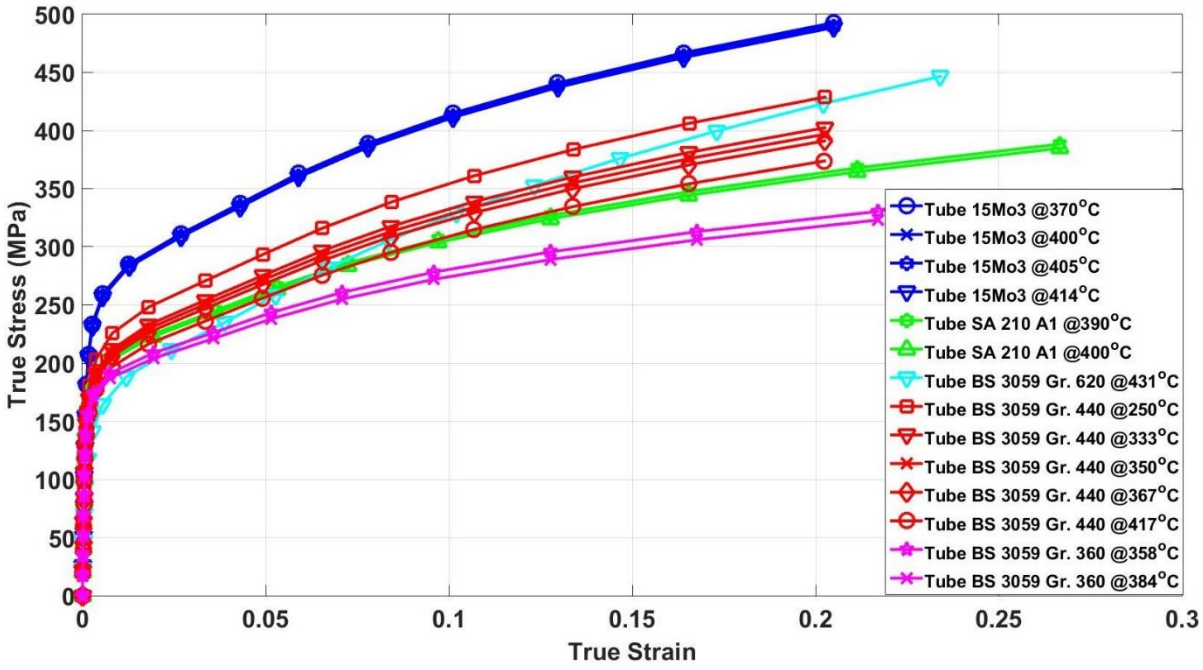

Fig. 1. Stress-strain curves for the boiler tubes at their corresponding operating temperatures.

2.2 Flaw geometry and parameterization

The flaw geometries of the tubes are modeled using our previously developed mathematical formulations that can accurately replicate the flaw dimensions (length, f_l, width, f_w and depth, f_d) of a wide range of localized erosion flaws [6]. Using the DesignModeler tool in ANSYS®, the flaws are designed to be in form of convex elliptical shape (*scoop-shaped*) or concave elliptical shape (*saddle-shaped*) as shown in Fig. 2. A detailed description of how to construct the flaw shapes can be found in our paper [6].

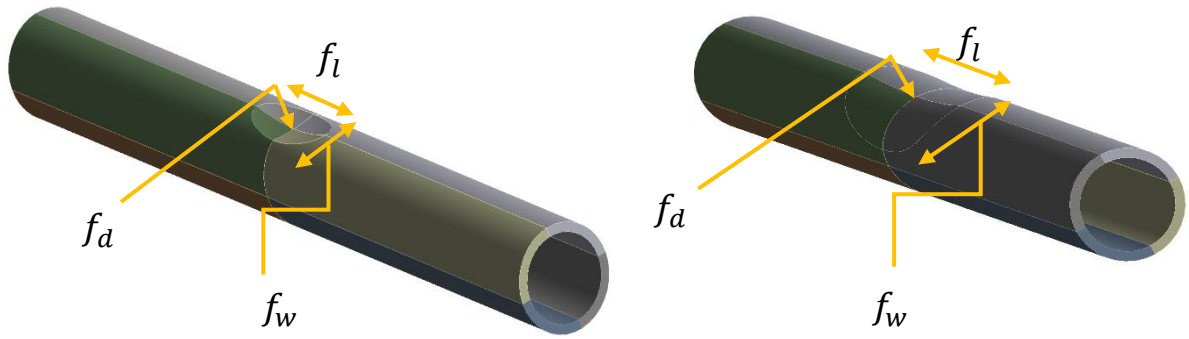

Fig. 2. An example of the modeled (a) Convex elliptical (scoop-shaped) flawed tube and (b) Concave elliptical (saddle-shaped) flawed tube.

Considering that all the defected tubes modeled in this study failed while in use, additional tubes with remaining wall thickness exceeding the remaining thickness of the failed tubes, t_f, are modeled via parameterization. For each failed tube, nine new models with identical flaw and tube dimensions, but varying remaining wall thickness are modeled from t_f to t_{min} (the minimum required uniform tube thickness that results in the allowable stress, σ). This implies above t_{min}, the safety of the tube can be assured, but below it, inelastic deformation is likely to commence. So, it is appropriate to investigate the analysis these tubes from t_{min}. The t_{min} values used for the modeling are computed using

$$t_{min} = \frac{PD_o}{2\sigma+P} \quad (1)$$

which is obtained from BS 1113-1999 [31]. D_o is the actual external diameter of the tube. The t_{min} is computed based on the internal pressure and allowable stress, in the absence of any additional stresses. The allowable stress, σ values at the operating temperature are obtained from the ASME and British design standards [28,31] are shown in Table 4. For 15 Mo3 tubes, their equivalence σ in the BS 3059 standard is used. The computed values of t_{min} are substantially less than the thickness of the unflawed tube, *t*, as expected. Through parameterizing the flaw geometries, a total of 160 models are generated and used for the analysis.

Table 4

Boiler tube minimum required thickness, t_{min} based on allowable stress, σ.

Flaw numbers	Tube grades	P (MPa)	D_o (mm)	σ (MPa) at T	t_{min} (mm)	t (mm)
1	15Mo3	21.81	44.5	118.80	3.74	5.6
2	15Mo3	19.40	33.9	117.00	2.60	6.5
3	*15Mo3	19.00	44.5	116.80	2.80	5.2
4	15Mo3	20.91	33.0	116.44	2.72	3.6
5	SA 210 A1	17.50	50.8	95.37	4.27	6.3
6	SA 210 A1	19.58	47.5	89.03	4.71	5.4
7	BS 3059 Gr. 620	12.10	34.9	117.52	1.71	4.2
8	BS 3059 Gr. 440	20.00	38.0	134.00	2.64	3.8
9	BS 3059 Gr. 440	12.10	63.5	110.42	3.30	6.1
10	BS 3059 Gr. 440	11.20	63.0	106.00	3.16	5.4
11	BS 3059 Gr. 440	20.21	38.0	104.30	3.36	3.8

12	BS 3059 Gr. 440	20.21	38.0	104.30	3.36	3.8
13	BS 3059 Gr. 440	20.35	63.5	100.30	5.85	6.6
14	BS 3059 Gr. 360	12.00	50.8	85.56	3.33	4.4
15	BS 3059 Gr. 360	12.40	50.8	85.56	3.43	4.4
16	BS 3059 Gr. 360	12.40	75.0	80.88	5.34	7.0

*Due to the nature of the flaw, a reduced t_{min} that is sufficient for the flaw is used.

2.3 Mesh, loads and boundary conditions

By implementing symmetry conditions, a quarter of the model can be used for the analysis. The flaw area is partitioned along the longitudinal direction to enhance the ease of applying mesh control procedures within it. Twenty-node quadratic hexahedral elements are used for the global meshing of the modeled tubes, with edge lengths approximately 2 mm. These are applied on the tube in the longitudinal and transverse directions. Local mesh controls (body size, multizone, hex dominant and a vertex sphere of influence applied at the minimum tube thickness t_r) are used to create finer quadratic hexahedral meshes within the flaw area, the outer part being 1 mm in size and then around the edge of the flaw area, 0.125 mm in size (see Fig. 3). Edge sizing control is also applied on the edge of the remaining thickness of the tube (t_r), to create five elements through the thickness of the tube. Fig. 4 shows examples of the meshed localized areas of the scooped-shaped flaw and that of the saddled-shaped flaw. The application of these mesh controls enhances the mesh quality of each model and ensures accurate results are obtained from the simulation. The total number of nodes and elements for the models ranges from 67,551 nodes and 11,801 elements, with an average aspect ratio of 2.239 for the tube with the smallest flaw to 441,118 nodes and 92,957 elements, with an average aspect ratio of 1.789 for the tube with the longest flaw.

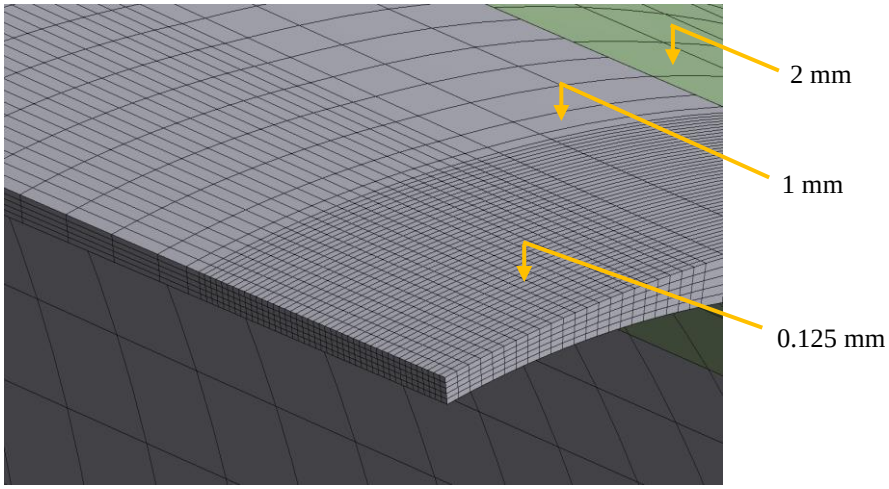

Fig. 3. Various sizes of the elements used for the meshing of the tube.

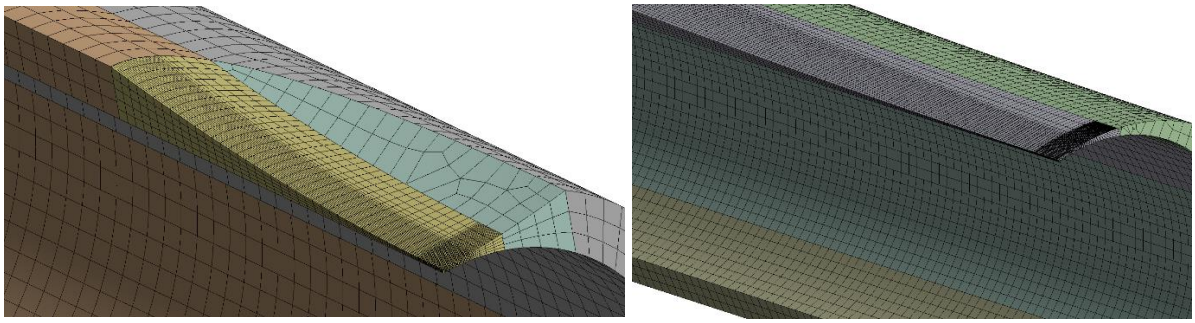

Fig. 4. Meshed localized areas for (a) scoop-shaped flawed tube and (b) saddle-shaped flawed tube.

On the symmetry boundaries of the models, frictionless supports are employed. A remote displacement constraint is fixed at the edges of the model to restrict it from rotating and translating, except in the vertical direction as shown in Fig. 5. The pressure is ramped up to the operating pressure, P. For end cap effects, an axial force, F, computed from the internal pressure P, is applied at the end of the models. Notice that this assessment is implicitly validated by carrying out the analysis at the respective operating pressures at which the tubes failed.

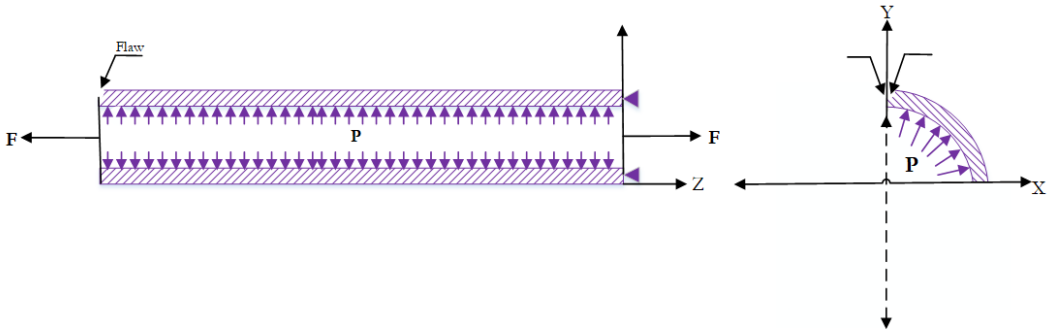

Fig. 5. Boundary conditions and load applied on the quarter model.

2.4 Finite element analysis of the tubes using various failure criteria

Nonlinear static structural analysis is performed on the modeled tubes, evaluated based on their respective operating pressures. The models are solved using initial and minimum sub-steps of 20 and maximum steps of 1000 in ANSYS® mechanical platform. Each simulation is run to the point of failure, which occurs when the analysis code does not converge because of plastic strain localization within the model, comparable to necking that occurs in a tensile test. The maximum von Mises stress and plastic strain for each modeled tube occur where the wall thickness is at its minimum. These values are solved as the applied pressure increases.

Fig. 6 shows the obtained maximum von Mises stress normalized by σ_{uts} for the percentage tube remaining thickness, $(t_r/t)\%$. Notice that almost all the flawed tubes failed once the maximum von Mises stress exceeded σ_{uts}. This correlates with prior studies on localized eroded pipes that recommended using σ_{uts} as the failure criteria limit [17,19]. However two tubes (Flaw 4 and Flaw 6), failed below σ_{uts}. Based on this, we rather recommend 0.9 σ_{uts} or 0.8 σ_{uts} as a more appropriate reference failure stress to be used. The plot of the maximum equivalent plastic strains against the percentage remaining wall thickness, $(t_r/t)\%$, can be seen in Fig. 7. For all the tube grades and flaw geometries, maximum equivalent plastic strains range from about 7% to 23%. The obvious implication is that all these tubes would survive at least up to 6% plastic strain before eventually failing. This is in line with previous studies that postulated a 2% plastic strain ($P_{2\%}$) limit for analyzing the failure of pressure vessels under localized thinning [15,32]. On a general note, most of these tubes failed at wall thickness below 20% of the unflawed wall thickness, except for Flaw 11 and Flaw 6 that failed at 21.3% and 22.2% respectively.

Plastic strain and stress criteria (0.9 σ_{uts}, 0.8 σ_{uts}, 2% plastic strain ($P_{2\%}$), and 5% plastic strain ($P_{5\%}$), all obtained from previous studies - [12,15,17,19,32]) were used in analyzing the plastic

strain and von Mises stress response. The tube remaining thickness, t_r at these limits were higher than the remaining thickness of the failed tube, t_f. If we take an instance of using the 0.8 σ_{uts} limit, the predicted remaining tube thickness that could be considered safe for Flaw 7 is 0.51 mm (12% t), which exceeds the actual remaining thickness of the failed tube, 0.20 mm (5% t). Equally, if we rather use the $P_{5\%}$ limit, the predicted tube remaining thickness before failure for Flaw 7 is 0.60 mm (14% t), which also exceeds the actual remaining thickness of the failed tube. Hence, any of these criteria could be used for the failure prediction of the tubes.

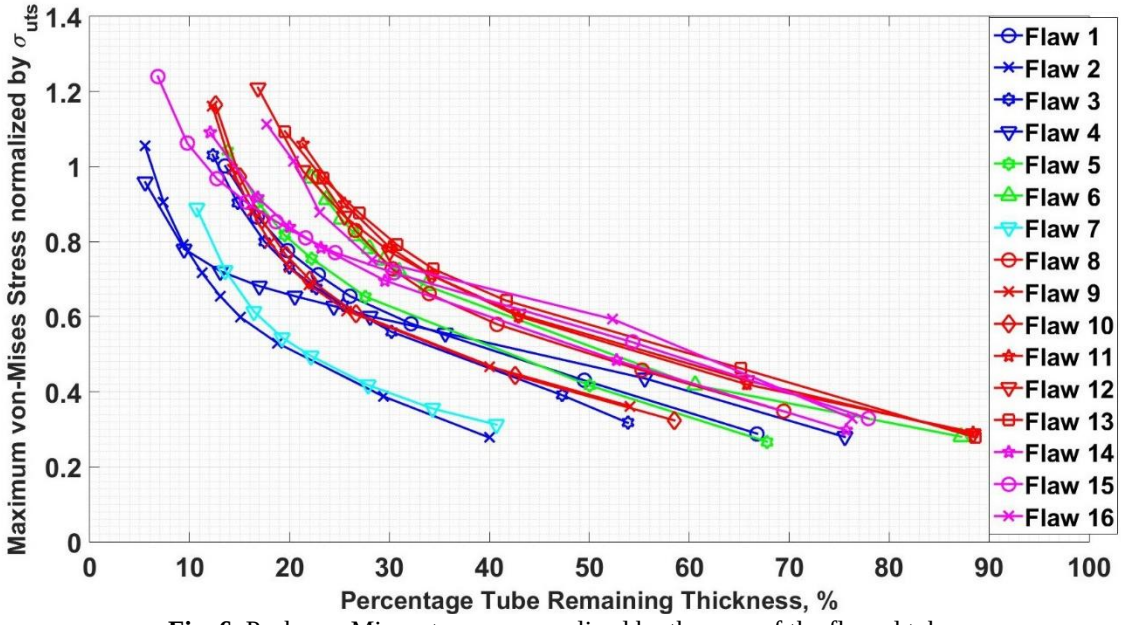

Fig. 6. Peak von Mises stresses normalized by the σ_{uts} of the flawed tube.

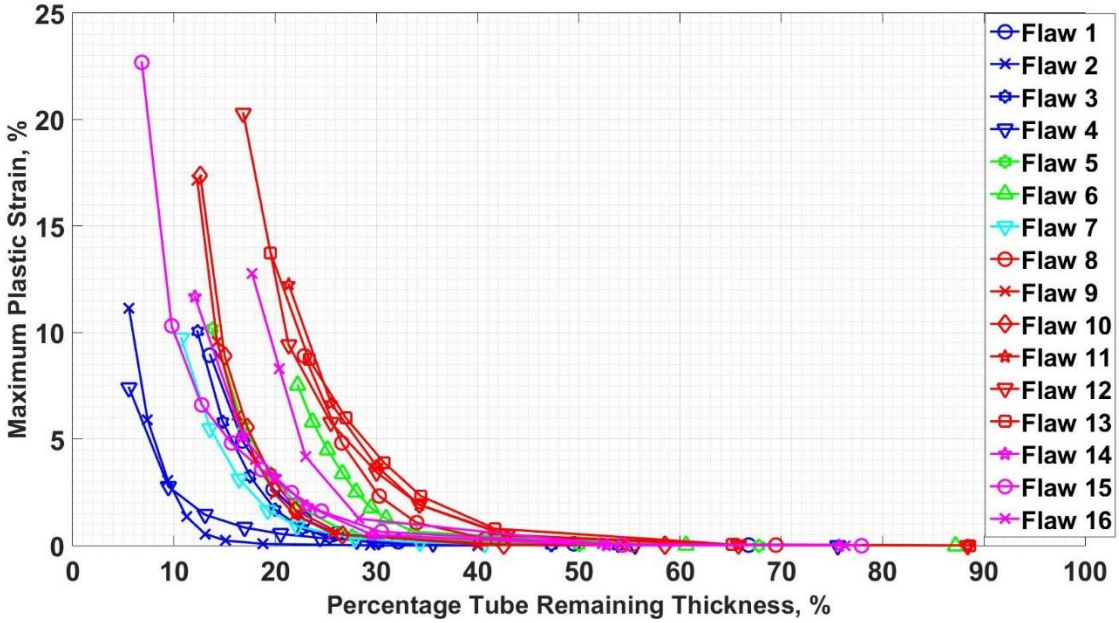

Fig. 7. Peak plastic strains of the flawed tubes.

In this section, assessment on tubes with localized external erosion flaws was performed using the tube and flaw dimensions, and their operating pressures and temperatures. Following this procedure, a user can generate von Mises and plastic strain curves for various tube grades to be assessed, and based on the stress or strain limit used, predicted values of the remaining thickness of the tubes can easily be obtained. Next, we compare the outcome of the assessment conducted to the API-ASME FFS assessment and also compute the projected time to failure of the tubes.

3 Comparing tube assessment with API-ASME FFS method

Using the elastic-plastic stress analysis method of the API-ASME FFS standard [27], fitness-for-service (FFS) assessment was carried out on the 160 models used for this study. A detailed description on how to conduct the FFS assessment is contained in our previous paper [12]. In this paper, we focus on comparing the outcomes from the analysis of the tubes using various failure criteria with respect to that of the API-ASME assessment outcomes.

Factored loads as stated in the API-ASME standard [27] and as shown in Table 5 are used to perform the FFS assessment. To perform elastic-plastic stress analysis on the tubes under internal pressure only, the required factored load combinations as shown in Table 5 are used. β is the factored load coefficient which varies for different construction codes and RSF_a is the allowable remaining strength factor, which has a recommended value of 0.9 based on the standard. The EN 13345 and PD5500 codes are used respectively for the 15Mo3 and BS 3059 tubes studied in this paper. The ASME Section VIII, Division 2 code can be applied for all flawed tubes, especially the SA 210 tubes. It should be noted that the load factors are the maximum values that should be used to first run the model but when the model does not converge, the load factors are either reduced or the tube remaining thickness increased until convergence is attained. While ensuring protection against plastic collapse (global stability) of

the tubes by using the factored loads, local stability (protection against local failure) is also fulfilled by ensuring the simulation is done within the strain limit specified in the standard. The process is time-consuming, as it may require many simulations that will not converge, thereby consuming a lot of computational resources and time.

Table 5
Load factor combinations used for the FFS assessment extracted from the API-ASME FFS standard [27]

Boiler Tube Construction Code	β	Required Factored Load (βP)
ASME VIII, Div. 2, 2007 Edition and Later (ASME)	$2.40RSF_a$	$2.16P$
EN 13345 (EN)	$2.40RSF_a$	$2.16P$
PD 5500 (BS)	$2.35RSF_a$	$2.12P$

Table 6 shows the result of the predicted tube remaining thickness at failure (t_{pf}) using different failure criteria. The predicted thicknesses at the limit of serviceability (t_{ps}) are also determined from the FFS analyses. These are compared to the measured minimum wall thickness of the failed tubes (t_f). It can be seen that the plastic strain- and stress-based failure criteria predicted wall thickness values are less conservative compared to those of the FFS approach. This is expected since the flaw depth at which the tube reaches the limit of serviceability is smaller than the flaw depth at which final failure occurs. The FFS result based on the ASME VIII, Div. 2, 2007 Edition and Later (ASME) and the EN 13345 (EN) load factors give the most conservative result. Again, since below t_{min}, plasticity (inelastic deformation) is likely to set in, 0.9 t_{min} was used as the onset of plasticity. This is different from the thickness at which numerical failure is observed. Fig. 8 shows the effect of comparing the normalized predicted values for each tube using the ASME/EN (t_{pf}/t_{ps}(ASME/EN)) result for the percentage tube remaining thickness at the onset of plasticity (0.9 t_{min}/t)%. It will be seen from the figure that the $P_{2\%}$ strain limit predicted values are between 0.63 – 1.05 of ASME/EN. Those obtained using the $P_{5\%}$ strain limit are 0.48 – 0.70 (ASME/EN), while values from the 0.8 σ_{uts} and 0.9 σ_{uts} limits are (0.59 – 0.80 of ASME/EN) and (0.49 – 0.63 of ASME/EN) respectively. The BS prediction values are between 0.93 – 0.98 (ASME/EN).

Table 6

Predicted tube remaining thickness at failure, t_{pf} and at limit of serviceability, t_{ps} using various failure criteria and the FFS

Flaw numbers	Tube grades	t_f (mm)	t_{pf}, $P_{2\%}$ (mm)	t_{pf}, $P_{5\%}$ (mm)	t_{pf}, 0.9 σ_{uts} (mm)	t_{pf}, 0.8 σ_{uts} (mm)	t_{ps}, ASME/EN (mm)	t_{ps}, BS (mm)
1	15Mo3	0.41	1.18	0.94	0.90	1.06	1.64	1.60
2	15Mo3	0.24	0.69	0.53	0.49	0.60	0.82	0.80
3	15Mo3	0.50	1.01	0.82	0.77	0.91	1.40	1.37
4	15Mo3	0.20	0.42	0.28	0.25	0.32	0.40	0.37
5	SA 210 A1	0.38	1.38	1.11	1.10	1.28	2.00	1.96
6	SA 210 A1	1.20	1.56	1.33	1.30	1.47	2.49	2.43
7	BS 3059 Gr. 620	0.20	0.78	0.60	0.45	0.51	0.86	0.84
8	BS 3059 Gr. 440	0.45	1.18	1.00	0.94	1.05	1.79	1.76
9	BS 3059 Gr. 440	0.63	1.27	1.05	0.97	1.10	1.84	1.80
10	BS 3059 Gr. 440	0.42	1.16	0.96	0.89	1.01	1.71	1.66
11	BS 3059 Gr. 440	0.30	1.29	1.07	0.97	1.12	1.90	1.86
12	BS 3059 Gr. 440	0.30	1.29	1.03	0.93	1.09	1.85	1.80
13	BS 3059 Gr. 440	0.80	2.37	1.90	1.70	2.00	3.28	3.21
14	BS 3059 Gr. 360	0.17	1.00	0.75	0.77	0.98	1.43	1.36
15	BS 3059 Gr. 360	0.30	1.02	0.68	0.70	0.98	1.43	1.36
16	BS 3059 Gr. 360	0.50	1.88	1.58	1.60	1.84	2.83	2.77

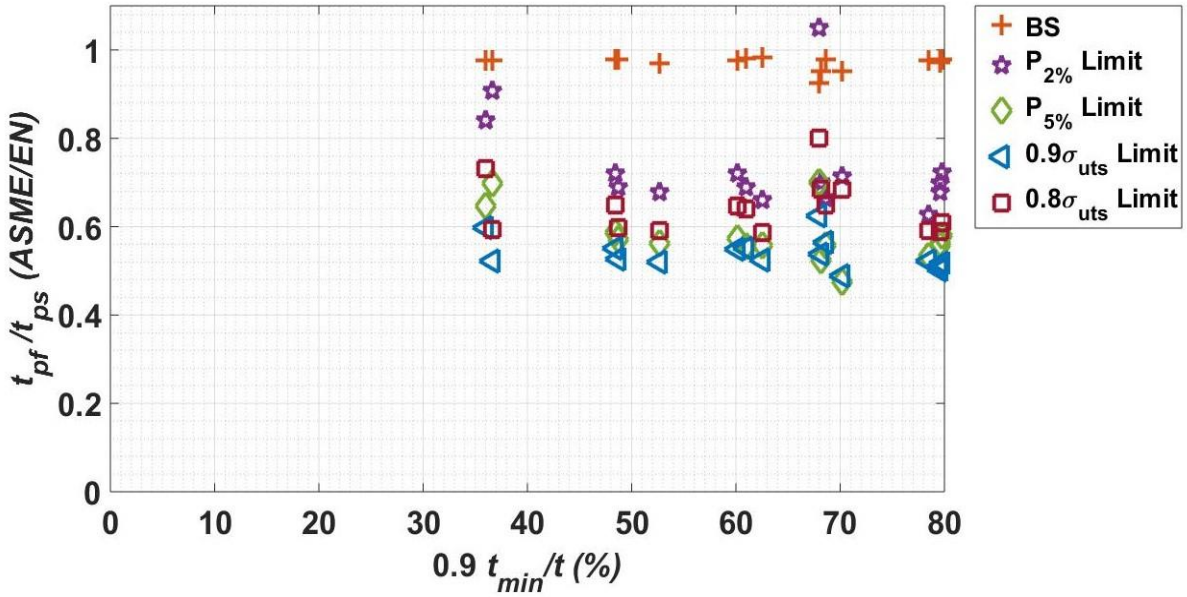

Fig. 8. Comparison with using various failure criteria and maximum load factors of the FFS assessment.

4 Computing the Projected Time to Failure of the Flawed Tubes

To aid industry users to make a judgment on the ranking of which flaws could be most critical, the remaining life of the tubes under investigation will have to be determined. The projected time to failure for each of the tubes will be the major determinant of which defected tubes have to be replaced or repaired as a priority. Thus, the projected time to failure for each tube based on the various criteria is computed from

$$P_t = \frac{t_t - t_p}{E_r} \quad (2)$$

where P_t is the projected time to failure of a tube experiencing localized erosion, t_t is the tube thickness at the time of assessment, t_p is the predicted tube remaining thickness obtained using any of the failure criteria or limit of serviceability and E_r is the estimated localized erosion rate of the tube.

In practice, erosion rates would be estimated from inspection reports for each specific flaw. In this study, we have assumed an erosion rate of 1 mm/year to demonstrate the idea of ranking the flaws. The projected time to failure (P_t) of the flawed tube can then be computed from the onset of plasticity ($0.9\ t_{min}$). Fig. 9 shows how we could use different failure criteria to prioritize the repairs of the tubes. The results of the projected time to failure (in years) for the percentage tube remaining thickness of each flawed tube at the onset of plasticity ($0.9\ t_{min}/t$)%, is depicted. Generally, for most of the flaws, the projected time to failure increases as the percentage tube remaining thickness increases. The stress based limit predictions has an average of 2.2 years, the strain based limits, 1.72 years, while those of the ASME/EN and BS standards have 1.46 mean years. Based on the time until the next shutdown, detected flaws can be properly ranked in terms of their level of criticality, with priority given to the one that will fail first.

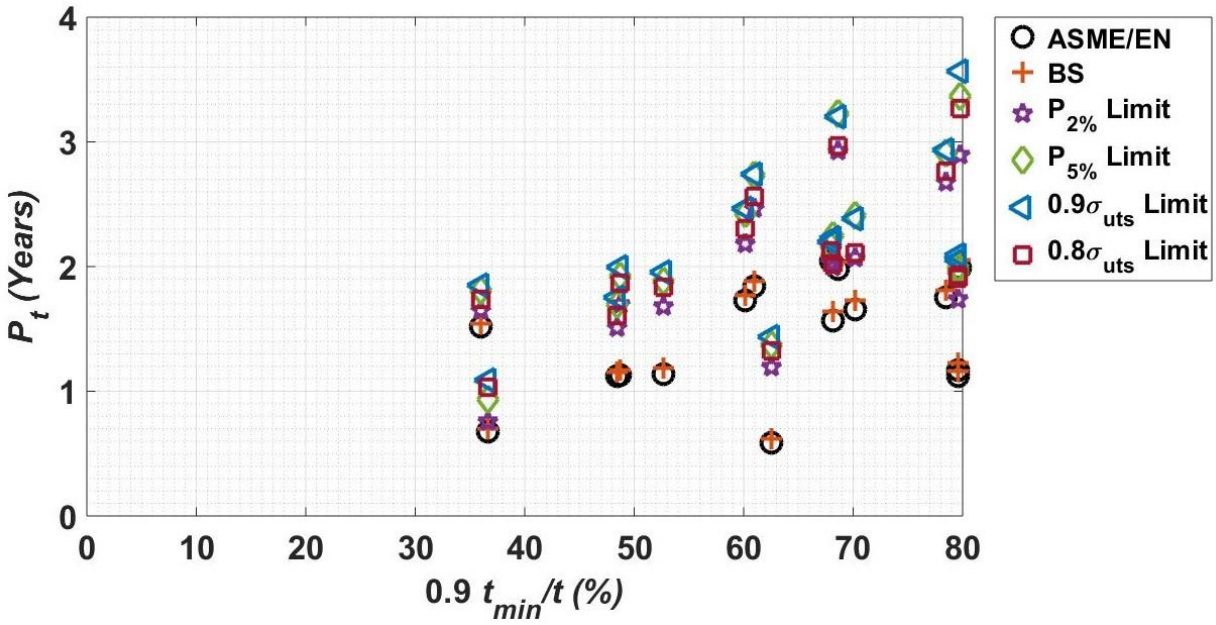

Fig. 9. Projected time to failure of the flawed tubes based on each failure criteria used.

Table 7 shows the ranking of the various flaws based on the criteria used. The ranking will vary depending on the failure criteria used for the prediction. For instance, Flaw 8 (with a percentage tube remaining thickness of 62.5%) will be predicted to fail ahead of Flaw 7 (with a percentage tube remaining thickness of 36.6%) using the ASME/EN and BS, while it is the other way round using the $P_{2\%}$ and other limits. The ranking of the tubes based on ASME/EN and BS tubes were the same, while those of the stress and strain limits were also quite similar. The projected time to failure or serviceability limits in hours of the flaws as seen in Table 8 also show a similar trend. Since the various criteria have been able to predict the tubes' failure before they occurred, this gives an industry user the flexibility of using any of the criteria depending on their maintenance budget and economic capacity.

Table 7

Ranking of flaws based on various failure criteria, in order of most urgent to least urgent to replace. Flawed tubes that need to be replaced within a year are color coded red and those that can extend beyond a year are color coded blue.

$P_{2\%}$	$P_{5\%}$	0.9 σ_{uts}	0.8 σ_{uts}	ASME/EN	BS
Flaw 7	Flaw 7	Flaw 7	Flaw 7	Flaw 8	Flaw 8
Flaw 8	Flaw 8	Flaw 8	Flaw 8	Flaw 7	Flaw 7
Flaw 3	Flaw 3	Flaw 3	Flaw 3	Flaw 3	Flaw 3
Flaw 2	Flaw 2	Flaw 2	Flaw 2	Flaw 11	Flaw 11
Flaw 10	Flaw 10	Flaw 10	Flaw 10	Flaw 9	Flaw 9
Flaw 9	Flaw 9	Flaw 9	Flaw 9	Flaw 10	Flaw 10

Flaw 11	Flaw 11	Flaw 11	Flaw 11	Flaw 12	Flaw 12
Flaw 12	Flaw 12	Flaw 12	Flaw 12	Flaw 2	Flaw 2
Flaw 14	Flaw 4	Flaw 4	Flaw 14	Flaw 14	Flaw 14
Flaw 4	Flaw 14	Flaw 14	Flaw 15	Flaw 15	Flaw 15
Flaw 15	Flaw 15	Flaw 15	Flaw 4	Flaw 1	Flaw 1
Flaw 1	Flaw 1	Flaw 1	Flaw 1	Flaw 6	Flaw 6
Flaw 5	Flaw 5	Flaw 5	Flaw 5	Flaw 5	Flaw 5
Flaw 6	Flaw 6	Flaw 6	Flaw 6	Flaw 16	Flaw 16
Flaw 13	Flaw 16	Flaw 16	Flaw 16	Flaw 13	Flaw 13
Flaw 16	Flaw 13	Flaw 13	Flaw 13	Flaw 4	Flaw 4

Table 8

Projected time to failure or limit of serviceability of each flawed tube in hours (h) based on various failure criteria

S/N	$P_{2\%}$ (h)	$P_{5\%}$ (h)	0.9 σ_{uts} (h)	0.8 σ_{uts} (h)	ASME/EN (h)	BS (h)
Flaw 1	19,149	21,252	21,602	20,201	15,120	15,470
Flaw 2	14,454	15,856	16,206	15,242	13,315	13,490
Flaw 3	13,228	14,892	5,330	14,104	9,811	10,074
Flaw 4	17,765	18,992	19,254	18,641	17,940	18,203
Flaw 5	21,576	23,941	24,029	22,452	16,145	16,495
Flaw 6	23,468	25,483	25,746	24,256	15,321	15,847
Flaw 7	6,649	8,226	9,540	9,014	5,948	6,123
Flaw 8	10,477	12,054	12,579	11,616	5,133	5,396
Flaw 9	14,892	16,819	17,520	16,381	9,899	10,249
Flaw 10	14,752	16,504	17,117	16,066	9,934	10,372
Flaw 11	15,190	17,117	17,993	16,679	9,846	10,197
Flaw 12	15,190	17,467	18,343	16,942	10,284	10,722
Flaw 13	25,360	29,477	31,229	28,601	17,389	18,002
Flaw 14	17,494	19,684	19,509	17,669	13,727	14,340
Flaw 15	18,107	21,085	20,910	18,457	14,515	15,129
Flaw 16	25,632	28,260	28,085	25,982	17,310	17,835

The outcome of this study provides a means of assessing boiler tubes with localized external erosion that could be relatively less time consuming to conventional assessment methods, save computational and economic resources, and failure of detected flaws can be predicted before they occur. Failure assessment of boiler tubes can be conducted using any of the failure criteria evaluated in this study and can be categorized from the most severe to the least severe based on their projected time to failure. This will enable only critical flaws to be replaced or repaired while tubes that can still be safe for continued service are left for the next scheduled outage. By so doing, it will help to mitigate unplanned outages and aid industries to judiciously use their maintenance budget.

5 Conclusions

This paper presents an assessment conducted on boiler tubes that failed as a result of localized external erosion. Nonlinear static structural analysis was carried out on tubes with a broad range of external erosion flaws, evaluated using various failure criteria and based on the operating pressures at which the tubes failed. The criteria were all able to predict the failure of the tubes earlier than they occurred. The predicted remaining thickness at failure for the tubes, t_{pf}, were higher than the remaining thickness of the failed tube, t_f, as expected. Comparing the outcomes of the analysis with the Fitness for Service (FFS) assessment using ASME, EN and PD/BS factored loads, the specific von Mises stress and that of the plastic strain limit, which correspond to the FFS ASME, EN, BS predictions were matched. It was observed that the predicted remaining tube thickness result at failure of the plastic strain and stress limits were relatively less conservative compared to the FFS predictions of the tube thickness at the limit of serviceability. To enable industry users to rank which flaws could be more critical than others, a projected time to failure (P_t) based on various criteria used in this study was computed for each tube. This enabled the proper ranking of the flaws based on how critical they were, from most severe to least severe so as to prioritize their repair or replacement.

The result from this study is encouraging to users in industry who would want to use a relatively less tedious and time-consuming means to assess the integrity of boiler tubes under localized erosion. It will also provide a user with the flexibility of choosing a less or more conservative failure criterion that may be considered suitable for different tube grades and scenarios, such as in an environment with ageing infrastructure and a constrained budget. Following the assessment conducted and presented in this paper, detected flaws can be ranked based on their level of criticality. This will enable industry users to prioritise the replacement or repair of only critical flawed tubes, prevent replacing the ones that can still continue in service, thereby averting unplanned outages that lead to production loss and high-cost urgent repairs.

Acknowledgements

The authors are grateful to the Department of Research and Innovation and the Centre for Asset Integrity Management at the University of Pretoria for their financial support and assistance towards this study. Sheda Science and Technology Complex (SHESTCO), Abuja, Nigeria is duly acknowledged for the leave granted to I. E. Kalu to undertake this study.

References

[1] B. Dooley, P.S. Chang, The current state of boiler tube failures in fossil plants, PowerPlant Chemistry. 2 (2000) 197–203.
[2] K. Zarrabi, H. Zhang, Creep and plastic collapse lives of scarred boiler tubes, Materials at High Temperatures. 15 (1998) 389–393.
[3] P. Haribhakti, P.B. Joshi, R. Kumar, Failure Investigation of Boiler Tubes: A Comprehensive Approach, ASM International, OH, USA, 2018.
[4] K. Zarrabi, Estimation of boiler tube life in presence of corrosion and erosion processes, International Journal of Pressure Vessels & Piping. 53 (1993) 351–358.
[5] S. Chaudhuri, Some aspects of metallurgical assessment of boiler tubes — Basic principles and case studies, Materials Science and Engineering A. 432 (2006) 90–99.
[6] I.E. Kalu, H.M. Inglis, S. Kok, The sensitivity of failure analysis of boiler tubes to the shape of elliptical external erosion flaws, Eng Fail Anal. 119 (2021) 1–16. https://doi.org/10.1016/j.engfailanal.2020.104952.
[7] Electric Power Research Institute (EPRI), Guidelines for control and prevention of fly ash erosion, CA, USA, 2011.
[8] ASM Handbook Committee, ASM Handbook, Volume 11, Failure Analysis and Prevention, ASM International, OH, USA, 2002.
[9] R.D. Port, H.M. Herro, The Nalco Guide to Boiler Failure Analysis by Nalco Chemical Company, McGraw-Hill, Inc, USA, 1991.
[10] M. Muscat, D. Mackenzie, R. Hamilton, A work criterion for plastic collapse, International Journal of Pressure Vessels and Piping. 80 (2003) 49–58.
[11] K. Zarrabi, H. Zhang, Primary stress in scarred boiler tubes, International Journal of Pressure Vessels and Piping. 65 (1996) 157–161.
[12] I.E. Kalu, H.M. Inglis, S. Kok, Failure assessment methodology for boiler tubes with localized external erosion defects, International Journal of Pressure Vessels and Piping. 188 (2020) 1–18. https://doi.org/10.1016/j.ijpvp.2020.104190.
[13] K. Zarrabi, A comparison of several boiler tube life prediction methods, International Journal of Pressure Vessels & Piping Vessels & Piping. 58 (1994) 197–201.
[14] J. Roy-Aikins, Challenges in meeting the electricity needs of South Africa, in: Proceedings of the ASME 2016 Power and Energy Conference (PowerEnergy2016-59085), 2016: p. V001T05A002.
[15] J.R. Sims, B.F. Hantz, K.E. Kuehn, A basis for the fitness for service evaluation, Pressure Vessel Fracture, Fatigue, and Life Management, ASME PVP. 233 (1992) 51–58.
[16] B.F. Hantz, J.R. Sims, C.T. Kenyon, T.A. Turbak, Fitness for service: Groove-like local thin-areas on pressure vessels and storage tanks, Plant Systems/Components Aging Management, ASME PVP. 252 (1993) 113–120.

[17] G. Fekete, L. Varga, The effect of the width to length ratios of corrosion defects on the burst pressures of transmission pipelines, Eng Fail Anal. 21 (2012) 21–30.
[18] J.E. Abdalla Filho, R.D. Machado, R.J. Bertin, M.D. Valentini, On the failure pressure of pipelines containing wall reduction and isolated pit corrosion defects, Comput Struct. 132 (2014) 22–33.
[19] B.N. Leis, D.R. Stephens, An alternative approach to assess the integrity of corroded line pipe - Part I : Current status, Proc. of the 7th International Offshore & Polar Eng. Conf. IV (1997) 624–634.
[20] Y. Kim, Y. Lee, W. Kim, K. Oh, The evaluation of failure pressure for corrosion defects within girth or seam weld in transmission pipelines, in: Proceedings of the International Pipeline Conference (IPC2004-216), Calgary, Alberta, Canada, October 4-8, 2004: pp. 1–9.
[21] J.B. Choi, B.K. Goo, J.C. Kim, Y.J. Kim, W.S. Kim, Development of limit load solutions for corroded gas pipelines, International Journal of Pressure Vessels and Piping. 80 (2003) 121–128.
[22] M. Kamaya, T. Suzuki, T. Meshii, Failure pressure of straight pipe with wall thinning under internal pressure, International Journal of Pressure Vessels and Piping. 85 (2008) 628–634. https://doi.org/10.1016/j.ijpvp.2007.11.005.
[23] J.W. Kim, C.Y. Park, S.H. Lee, Local failure criteria for wall-thinning defect in piping components based on simulated specimen and real-scale pipe tests, in: 20th International Conference on Structural Mechanics in Reactor Technology (SMiRT 20), Espoo, Finland, August 9-14, 2009: pp. 1–14.
[24] B. Ma, J. Shuai, D. Liu, K. Xu, Assessment on failure pressure of high strength pipeline with corrosion defects, Eng Fail Anal. 32 (2013) 209–219.
[25] I. Klevtsov, H. Tallermo, T. Bojarinova, A. Dedov, Assessment of remaining life of superheater austenitic steel tubes in oil shale PF boilers, Oil Shale. 23 (2006) 267–274.
[26] British Standards Institution (BSI), BS 3059: Part 2:1990 British Standard on Steel boiler and superheater tubes, 1990.
[27] American Petroleum Institute (API) and the American Society of Mechanical Engineers (ASME), Fitness-For-Service API 579-1/ASME FFS-1, Washinghton, D.C., USA, 2016.
[28] The American Society of Mechanical Engineers (ASME), ASME Boiler and Pressure Vessel Code, Section II, Part D: Materials Properties, 2017.
[29] G. Dini, S. Mahmoud, M. Vaghefi, M. Lotfiani, Computational and experimental failure analysis of continuous-annealing furnace radiant tubes exposed to excessive temperature, Eng Fail Anal. 15 (2008) 445–457.
[30] H. Othman, J. Purbolaksono, B. Ahmad, Failure investigation on deformed superheater tubes, Eng Fail Anal. 16 (2009) 329–339.
[31] British Standards Institution (BSI), Specification for design and manufacture of water-tube steam generating plant (including superheaters, reheaters and steel tube economizers) - BS 1113-1999, British Standards Institution, 2000.
[32] T.A. DePadova, J.R. Sims, Fitness for Service - Local thin areas comparison of finite element analysis to physical test results, Fitness-for-Service and Decisions for Petroleum and Chemical Equipment, ASME PVP. 315 (1995) 285–292.